Asia-Pac. J. Atmos. Sci., 52(2), 209-222, 2016
DOI:10.1007/s13143-016-0020-1
pISSN 1976-7633 / eISSN 1976-7951

Future Changes in Drought Characteristics over South Korea Using Multi Regional Climate Models with the Standardized Precipitation Index

Yeon-Woo Choi[1], Joong-Bae Ahn[1], Myoung-Seok Suh[2], Dong-Hyun Cha[3], Dong-Kyou Lee[4], Song-You Hong[5], Seung-Ki Min[6], Seong-Chan Park[7], and Hyun-Suk Kang[8]

[1]*Department of Atmospheric Sciences, Pusan National University, Busan, Korea*
[2]*Kongju National University, Kongju, Korea*
[3]*Ulsan National Institute of Science and Technology, Ulsan, Korea*
[4]*Seoul National University, Seoul, Korea*
[5]*Korea Institute of Atmospheric Prediction Systems, Seoul, Korea*
[6]*Pohang University of Science and Technology, Pohang, Korea*
[7]*Korea Meteorological Administration, Seoul, Korea*
[8]*National Institute of Meteorological Sciences, Jeju, Korea*

(Manuscript received 31 October 2015; accepted 15 April 2016)
© The Korean Meteorological Society and Springer 2016

Abstract: In this study, the projection of future drought conditions is estimated over South Korea based on the latest and most advanced sets of regional climate model simulations under the Representative Concentration Pathway (RCP4.5 and RCP8.5) scenarios, within the context of the national downscaling project of the Republic of Korea. The five Regional Climate Models (RCMs) are used to produce climate-change simulations around the Korean Peninsula and to estimate the uncertainty associated with these simulations. The horizontal resolution of each RCM is 12.5 km and model simulations are available for historical (1981-2010) and future (2021-2100) periods under forcing from the RCP4.5 and RCP8.5 scenarios. To assess the characteristics of drought on multiple time scales in the future, we use Standardized Precipitation Indices for 1-month (SPI-1), 6-month (SPI-6) and 12-month (SPI-12). The number of drought months in the future is shown to be characterized by strong variability, with both increasing and decreasing trends among the scenarios. In particular, the number of drought months over South Korea is projected to increase (decrease) for the period 2041-2070 in the RCP8.5 (RCP4.5) scenario and increase (decrease) for the period 2071-2100 in the RCP4.5 (RCP8.5) scenario. In addition, the percentage area under any drought condition is overall projected to gradually decrease over South Korea during the entire future period, with the exception of SPI-1 in the RCP4.5 scenario. Particularly, the drought areas for SPI-1 in the RCP4.5 scenario show weakly positive long-term trend. Otherwise, future changes in drought areas for SPI-6 and SPI-12 have a marked downward trend under the two RCP scenarios.

Key words: Regional climate model, climate change, IPCC RCP scenario, South Korea, drought

1. Introduction

A drought generally originates from a prolonged absence or deficiency of precipitation. Its potential to cause significant damage to agriculture, economy, and society worldwide has attracted research attention (Dai et al., 2004; Dai, 2011; Blenkinsop and Fowler, 2007; Solomon et al., 2007). Therefore, projections of future climate change associated with the intensity or duration of drought need to be estimated not only to understand how drought patterns are affected by increasing greenhouse gas (GHG) concentration but also to cope with natural disasters. Thus far, many previous studies have addressed the issue of projected changes in the hydrological cycle with global climate models (Hulme et al., 1994; Kim and Byun, 2009, Giorgi et al., 2011; Lee et al., 2014). Hulme et al. (1994) have reported that precipitation over most of the East Asia region is projected to increase during all seasons in response to a doubled CO_2 scenario using seven GCM results. They show that the strong warming signal over East Asia will be distinctly coupled with intensified monsoonal precipitation in the future. Using 15 GCM results for SRES A1B scenario, Kim and Byun (2009) have also shown that a large increase in mean precipitation is expected in the future, particularly in Asian monsoon regions, which will reduce drought over the region.

Furthermore, studies using high-resolution modeling systems are also being actively conducted. Since the spatial resolution of GCMs is too coarse to obtain fine-scale climate information, regional climate modeling is necessary to improve our understanding of regional climate processes associated with crop, plant phenology, and drought (e.g., Im et al., 2012; Lee and Hong, 2014; Hur and Ahn, 2014, 2015; Ahn et al., 2015). On the basis of regional climate model simulations using Regional Climate Model (RegCM) version 3 (Pal et al., 2007), Im et al. (2012) have pointed out that enhancement of the evapotranspiration under the background of global warming gives rise to the water stress in South Korea. Using the Regional Model Program (RMP) of the Global/Regional Integrated Model system (GRIMs; Hong et al., 2013), which has been used in several studies in order to understand the precipitation

Corresponding Author: Joong-Bae Ahn, Department of Atmospheric Sciences, Pusan National University, Jangjeon 2-dong, Geumjeong-gu, Busan 46241, Korea.
E-mail: jbahn@pusan.ac.kr

mechanisms over Asian monsoon region (Kang and Hong, 2008; Hong et al., 2012), Lee et al. (2014) have shown that the frequency and variability of heavy precipitation over East Asia will increase under the Representative Concentration Pathway 8.5 (RCP8.5) scenario, while the projected precipitation given by the RCP4.5 simulation is similar to those of the current climate. Several studies have also shown that the precipitation over East Asia will increase in the future based on single RCM assessments (Oh et al., 2014; Im et al., 2015; Hong and Ahn, 2015). However, it is difficult to reliably assess the future climate change using a single climate model because a variety of uncertainties produced by a single model are reflected in the model simulation. To reduce the uncertainty of future climate change, a Multi-Model Ensemble (MME) has been recommended (Krishnamurti et al., 1999; Yun et al., 2003). In line with this, the five Regional Climate Models (RCMs), including two hydrostatic RCMs (i.e., RegCM version 4 (RegCM4; Giorgi et al., 2012) and Regional Spectral Model (RSM; Hong et al., 2013)) and three non-hydrostatic RCMs (i.e., Weather Research and Forecasting model (WRF; Skamarock et al., 2005), Seoul National University Meso-scale Model version 5 (SNU-MM5; Lee et al., 2004; Cha et al., 2008) and Hadley Centre Global Environmental Model version 3 regional climate model (HadGEM3-RA; Davies et al., 2005)), are used to produce climate change projections over the Coordinated Regional Climate Downscaling Experiment (CORDEX) East Asia (Lee et al., 2014; Oh et al., 2014; Park et al., 2015).

Many previous studies have tried to project the intensity or duration of drought in the future by utilizing the MME system (Beniston et al., 2007; Blenkinsop and Fowler, 2007). Blenkinsop and Fowler (2007) have suggested that the MME from PRUDENCE RCMs predicts a significant change in European drought characteristics with different magnitudes and signs according to each region. Beniston et al. (2007) have shown that increased temperature under global warming could play an important role in modulating drought conditions based on the MME result from the PRUDENCE project.

In this study, we define the categories of drought according to their duration, such as climatological, agricultural, and hydrological drought using the standardized precipitation index (SPI; McKee et al., 1993). The majority of drought indices have a fixed time-scale, which does not allow identification of droughts, especially in shorter time scales, such as climatological and agricultural droughts. However, SPI is designed to quantify a precipitation deficit for different time scales (Guttman, 1998). The 1-month SPI (SPI-1, hereafter) denotes the climatological drought and 6- and 12-month SPIs (SPI-6 and SPI-12, hereafter) indicate agricultural and hydrological droughts, respectively. Thus far, however, insufficient studies have assessed the occurrences and trends of drought over South Korea using the MME obtained from the RCMs. The present study analyzes the drought characteristics in the future forced by the RCP4.5 and RCP8.5 scenarios using the MME from RCMs.

The paper is organized as follows. In Section 2, the data and model experimental design are briefly introduced and SPI and the consistency index are defined in detail. Section 3 evaluates the MME result for the current climate and future projection for precipitation. The projected change in drought is presented in Section 4. Finally, the study is summarized in Section 5.

2. Data and experimental design

a. Experimental design

In order to produce a high-resolution climate change scenario over South Korea, dynamical downscaling is conducted using five RCMs (GRIMs, HadGEM3-RA, RegCM4, SNU-MM5, WRF). The simulated results by the Hadley Centre Global Environmental Model version 2 - Atmosphere and Ocean (HadGEM2-AO; Collins et al., 2011; Baek et al., 2013) are used as the initial and lateral boundary conditions for the five RCMs. This climate model consists of the atmospheric General Circulation Model (GCM) with N96 ($1.875^{o} \times 1.25^{o}$) horizontal resolution and 38 vertical levels and ocean GCM with 1^{o} horizontal resolution and 40 vertical levels. According to the HadGEM2-AO CMIP5 results, the simulations exhibit better performance compared to other CMIP3 models, especially over India and the East Asia regions (Baek et al., 2013). Hong and Ahn (2015) have also shown that HadGEM2-AO shows a relatively good performance in simulating summer precipitation over Northeast Asia compared to CMIP5 MME. The results of HadGEM2-AO comprise the simulations of the Historical, RCP4.5, and RCP8.5 scenarios (HIS, RCP4.5, and RCP8.5, respectively, hereafter).

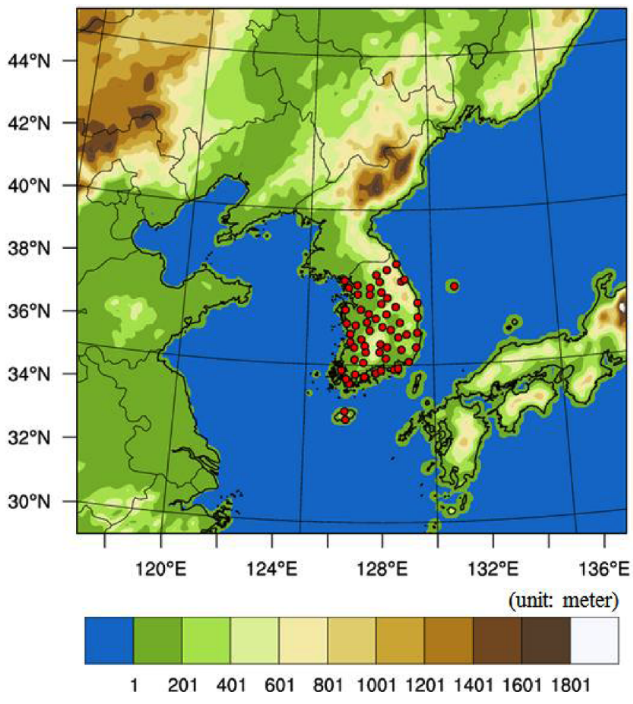

Fig. 1. Analysis domain and topography. The red dots denote the location of 60 weather stations over South Korea.

Table 1. List of Regional Climate Models (RCMs) and their configurations.

	GRIMs	HadGEM3-RA	RegCM4	SNU-MM5	WRF
Institute / Person in charge	POSTECH / S.-K. Min	NIMR / H.-S. Kang	KNU / M.-S. Suh	UNIST / D.-H. Cha	PNU / J.-B. Ahn
Horizontal resolution	182 × 201 (12.5 km)	180 × 200 (12.5 km)	180 × 200 (12.5 km)	180 × 200 (12.5 km)	180 × 201 (12.5 km)
Vertical coordinate/ levels	Sigma / 28	Hybrid / 38	Sigma / 23	Sigma / 24	Eta / 28
Dynamic framework	Hydrostatic	Non-hydrostatic	Hydrostatic	Non-hydrostatic	Non-hydrostatic
Convection scheme	SAS+CMT	Revised mass flux scheme	MIT-Emanuel	Kain -Fritsch II	Kain-Fritsch II
Land surface	OML climatology value	MOSES-II	CLM3.5	CLM3.0	Noah
LWR scheme	GSFC	Generalized 2-stream	CCM3	CCM2	CAM
SWR scheme	GSFC	Generalized 2-stream	CCM3	CCM2	CAM
Spectral nudging	Yes	No	Yes	Yes	No
References	Hong et al. (2013)	Davies et al. (2005)	Giorgi et al. (2012)	Cha and Lee (2009)	Skamarock et al. (2008)

The study is mainly performed for the South Korea domain (33°-38°N, 125°-130°E) based on the monthly-mean precipitation data from the ensemble of RCMs. The horizontal resolution of RCMs is 12.5 km and the model domain is centered at 37.5°N, 127.5°E (Fig. 1). For lateral boundary forcing, several grid points at each direction are used for the buffer zone, which is eliminated in estimating the projected climate changes for removing the possible impact of lateral boundary bias. A detailed description for the configuration of five RCMs is given in Table 1. Model simulations are available for HIS (1979-2010) and future (2019-2100) period under the RCP4.5 and RCP8.5 scenarios and the first two years (1979-1980 and 2019-2020) for each simulation is considered as the spin-up period. The 2041-2100 periods for the RCP4.5 and RCP8.5 scenarios are divided into two 30-yr time slices, 2041-2070 and 2071-2100, which respectively represent the near (Fut1, hereafter) and far (Fut2, hereafter) futures.

In order to reduce the uncertainty of future climate change, the MME is performed with equal weighting. The performance of the ensemble result from five RCMs is evaluated for the HIS experiment without removing the bias (Section 3a). The systematic model biases are partly eliminated in assessing the climate change by subtracting the climatological mean of the HIS experiment from those of the RCP experiment (Ahn et al., 2012, 2015; Hong and Ahn, 2015).

b. Observation data sets

The monthly-mean precipitation data set provided by the Asian Precipitation-Highly-Resolved Observational Data Integration Toward Evaluation (APHRODITE; Yatagai et al., 2012) project is used to evaluate the performance of the ensemble result from multi-RCMs. The period of this data set covers 25 years (1981-2005) because of the limited availability of data, the horizontal resolution of which is approximately 0.5° in both latitude and longitude directions over only land area. In order to validate the climate reproducibility of the RCMs in more detail, we use daily precipitation data from 60 weather stations (red dots in Fig. 1) over South Korea maintained by the Korea Meteorological Administration for the period 1981-2010.

Table 2. Standardized precipitation index (SPI) classification.

SPI values	Drought category
2.0 and above	Extremely wet
1.5 to 1.99	Very wet
1.0 to 1.49	Moderately wet
–0.99 to 0.99	Near normal
–1.00 to –1.49	Moderately dry
–1.5 to –1.99	Severely dry
< –2.0	Extremely dry

c. Definition of the Standardized Precipitation Index (SPI)

Many studies have tried to objectively define the threshold of drought by utilizing observation data. The SPI introduced by McKee et al. (1993) is currently the most widely used index (Hayes et al., 1999, 2011; Bothe et al., 2012; Trenberth et al., 2014), especially as a representative drought index, to monitor the meteorological drought by the World Meteorological Organization (WMO; Hayes et al., 2011). To investigate the projected changes in drought over South Korea, we define SPI (McKee et al., 1993). SPI is calculated by fitting a 2-parameter gamma distribution to monthly precipitation values, of which the classification scale is used to identify drought conditions (McKee et al., 1993; Table 2). We use the multiple time scale (1-month, 6-month and 12-month) SPIs (SPI-1, SPI-6 and SPI-12) to investigate the three types of drought (meteorological, agricultural and hydrologic) and define the threshold of

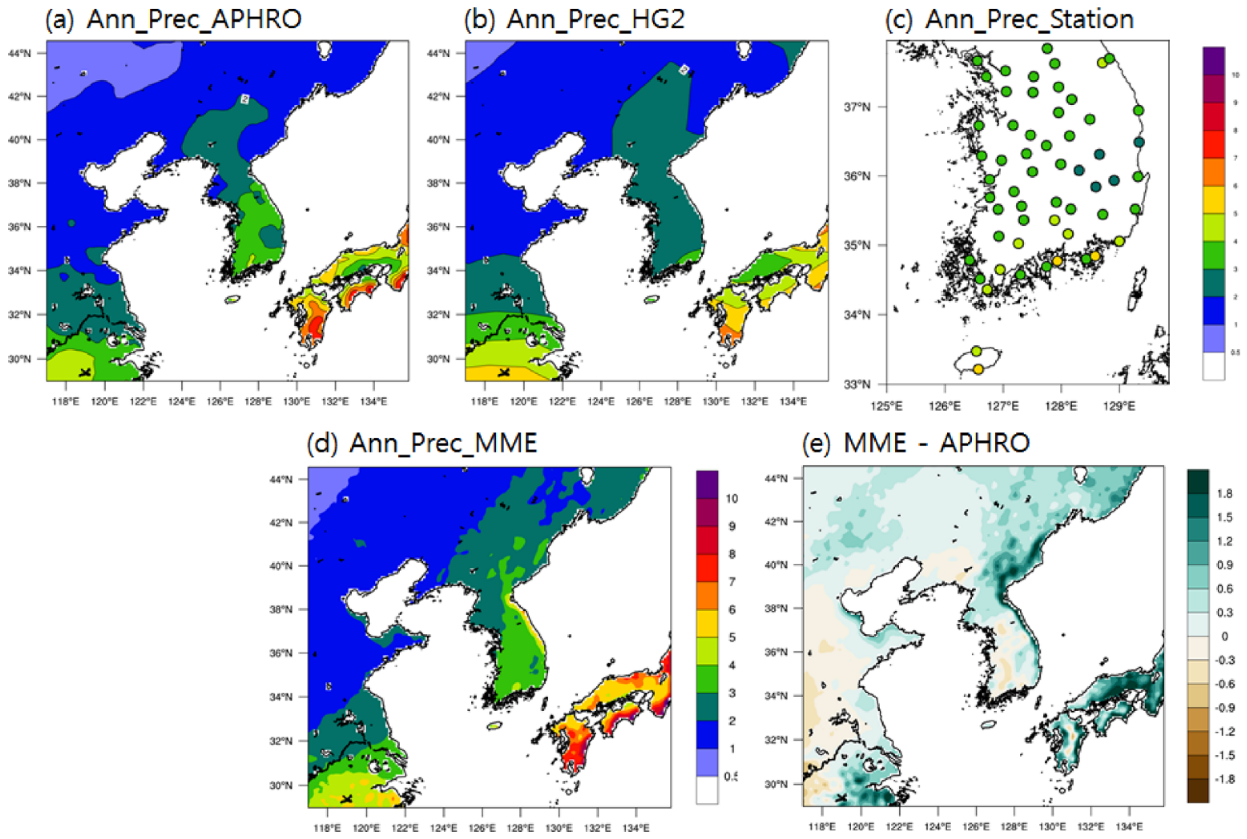

Fig. 2. Spatial distribution of annual mean precipitation (mm d^{-1}) for (a) APHRODITE, (b) HadGEM2-AO, (c) weather station data maintained by the Korea Meteorological Administration, (d) Ensemble of 5 RCMs, and (e) difference between Ensemble and APHRODITE. The period of data is 1981-2010 except for that of APHRODITE (1981-2005).

drought as values of SPIs less than −1.

d. Consistency index

In order to assess the level of consistency in annual-mean precipitation projected by 5 RCMs, we constructed a consistency index (Wang 2005; Kim and Byun, 2009). The index is calculated for each grid point as follows.

$$\text{Consistency index} = \begin{cases} \dfrac{Np}{Np+Nn}(Np>Nn) \\ -\dfrac{Nn}{Np+Nn}(Np<Nn) \end{cases}, \quad (1)$$

where Np is the number of RCMs that project an increase in precipitation, and Nn is the number of RCMs that predict a decrease. Therefore, the sign of the index denotes the direction of changes projected by the majority of the RCMs.

3. Results

a. Evaluation of Multi-Model Ensemble (MME) result

The performance of the MME in simulating the annual-mean precipitation during the HIS period (1981-2010) is evaluated over South Korea against both observations and the HadGEM2-AO. Figure 2 shows the climatology of the observed (APHRODITE, weather station data maintained by the Korea Meteorological Administration) and simulated (HadGEM2-AO, MME) annual-mean precipitation. The maximum precipitation with amounts greater than 6 mm d^{-1} is observed in southwestern Japan and a large amount of precipitation over South Korea and southeastern China is found in APHRODITE (Fig. 2a). The comparison between the MME obtained from the five RCMs and APHRODITE shows a similar spatial distribution of precipitation (Figs. 2a, d), whereas a large difference in precipitation over 0.9 mm d^{-1} appears in the highly mountainous region of the Korean peninsula (Fig. 2e). Overall, dry biases occur in the western part of South Korea, which are related to the bias from GCM simulation (Fig. 2b). Giorgi and Coppola (2010) reported that the projected regional climate change over East Asia is not significantly affected by model regional bias. In this regard, the systematic dry bias over the western part of South Korea can be eliminated by subtracting the climatological mean of the HIS from those of the RCP experiments. In addition, the difference in precipitation is relatively larger over western Japan and southeastern China than over South Korea; however, a discussion on this is beyond the scope of this study. The performance of HadGEM2-AO,

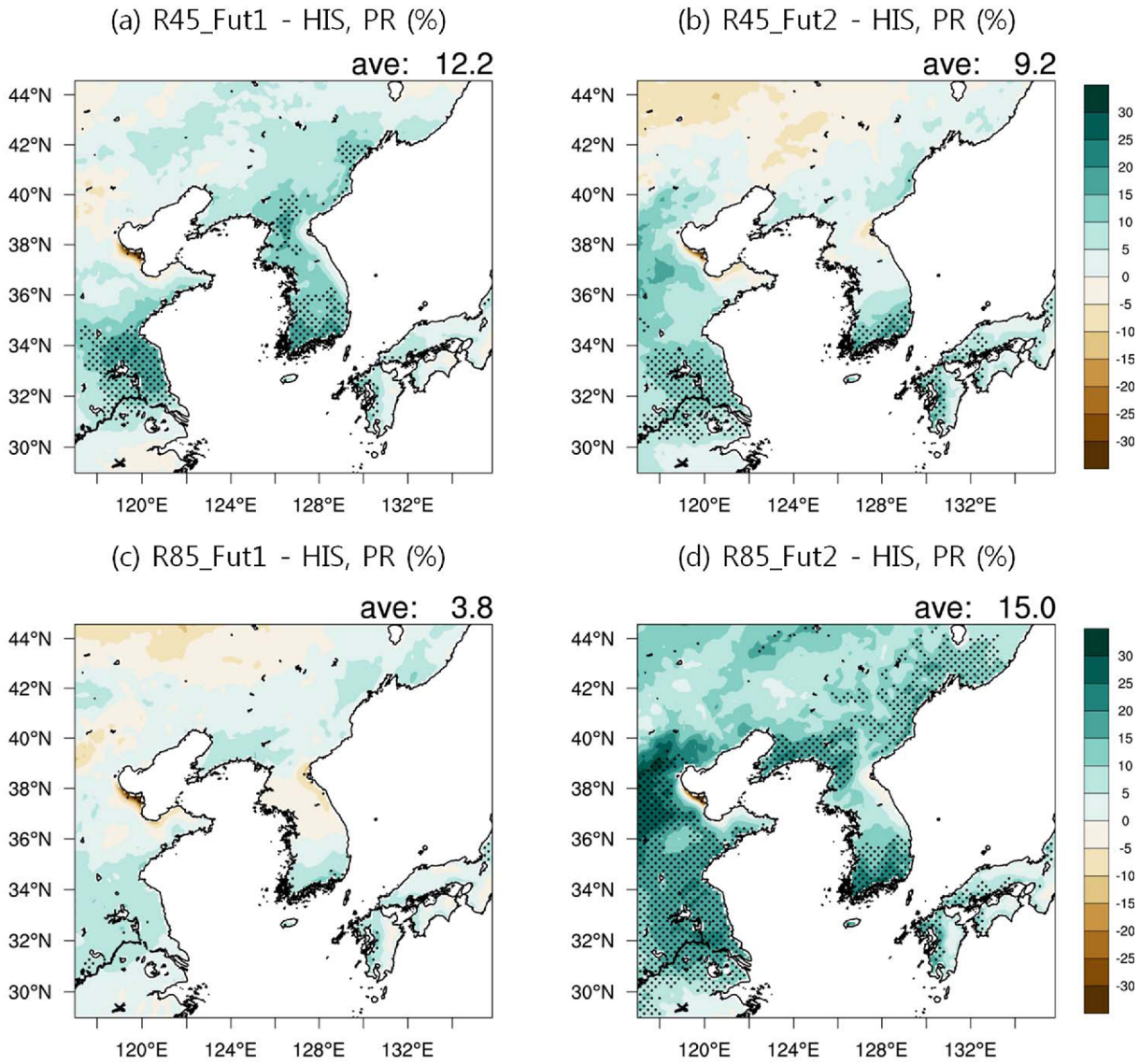

Fig. 3. Multi-model ensemble (MME) percentage differences in mean precipitation for (a, b) RCP4.5 and (c, d) RCP8.5 experiments during Fut1 (2041-2070) and Fut2 (2071-2100) periods against the historical (1981-2010) period. Superimposed black dots denote the areas where the changes are statistically significant at the 90% confidence level. The number at the top right of each panel indicates the annually averaged percentage differences of mean precipitation with respect to the historical period over South Korea.

used as large-scale forcing, is worse than that of the MME in simulating precipitation characteristics over the region because RCMs can produce added value, particularly in the regions where orographically-induced precipitation prevails (Lee and Hong, 2006, 2014). In order to validate the climate reproducibility of the RCMs in more detail, we compare simulated precipitation using the nearest grid point to the station location with the values of individual weather stations (Fig. 2c). The MME reproduces the observed spatial distribution of the precipitation over South Korea that is not depicted by HadGEM2-AO. These results provide an overview of the MME performance before projecting fine-resolution climate change on a regional scale.

b. Change in precipitation

Figure 3 shows the MME difference in mean precipitation (in percentage) for Fut1 and Fut2 periods against the HIS period under the two RCPs scenarios. The mean precipitation is projected to consistently increase over the southern part of South Korea (34°N-36°N). The significant increase in precipitation greater than 10% is observed over the same region and is significant at the 90% confidence level. Otherwise, the sign of projected precipitation change over the northern part of South Korea (36°N-40°N) differs depending on the period and the RCP scenarios. In particular, mean precipitation over the northern part of South Korea is projected to increase during

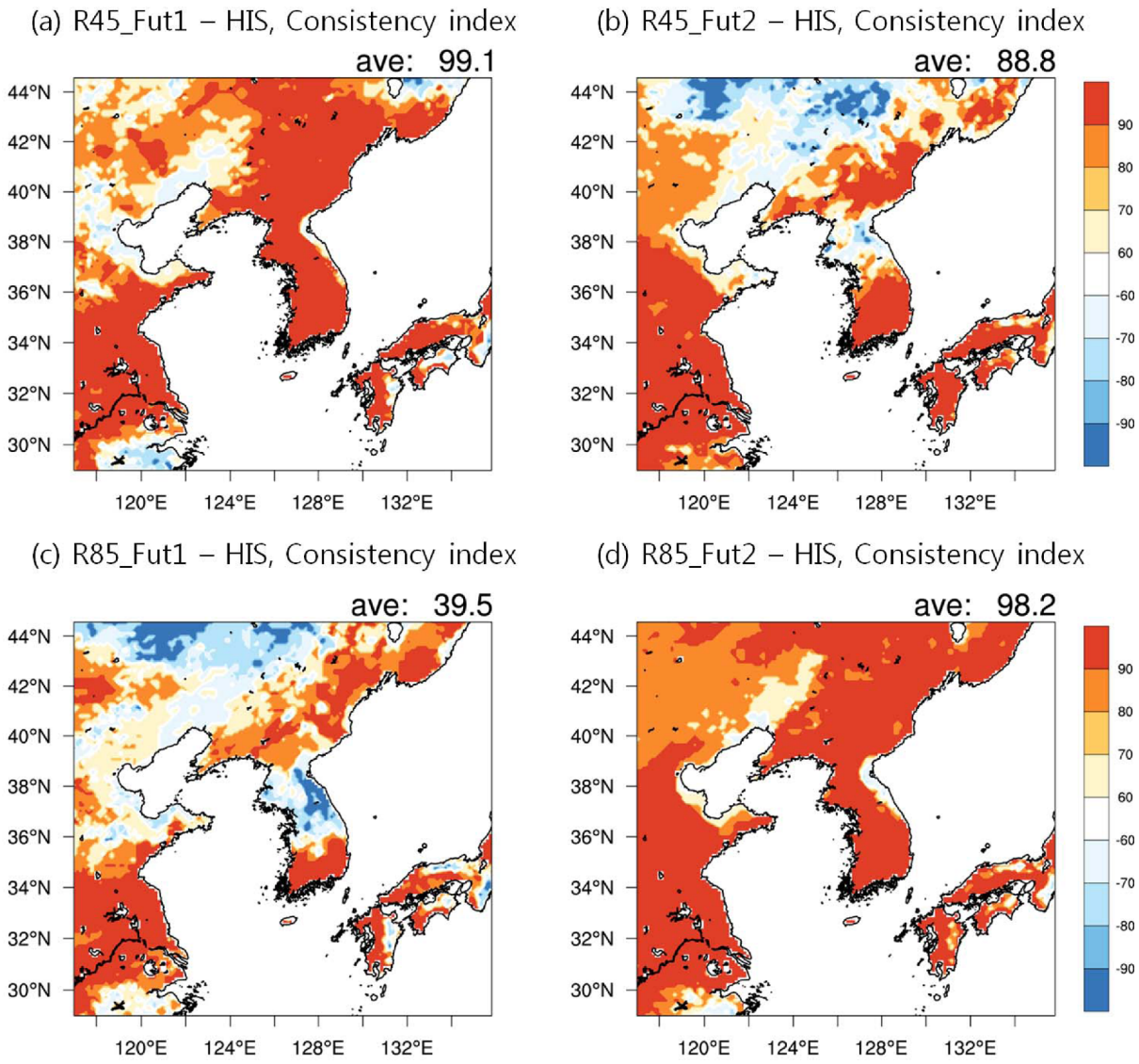

Fig. 4. Same as in Fig. 3 but for consistency index (unit: %).

Fut1 period in RCP4.5 and during Fut2 period in the RCP8.5 scenario, but decrease during Fut1 period in the RCP8.5 scenario and during Fut2 period in the RCP4.5 scenario. These differences in projected precipitation changes between the northern part of Korea and its surrounding regions are mostly due to the large variability of precipitation at decadal to multi-decadal scales. Many previous studies have described that regional-scale precipitation is characterized by decadal-to-multi-decadal scale variability, the structure of which varies markedly from region to region (Giorgi and Bi, 2005; Im et al., 2015). This feature is also supported from observational studies in the Korean peninsula. In previous studies using the weather station data, annual and seasonal mean precipitations in South Korea have a significant positive monotonic trend in the recent several decades (Chung and Yoon, 2000; Chung et al., 2004; Ko et al., 2005; Choi et al., 2010, 2013), whereas they have distinctive Inter-decadal variations over North Korea (Choi et al., 2010, 2013). One possible mechanism is that the recent decreasing tendency of rainfall in North Korea is caused by anomalous anticyclone, which is reinforced in regions near Lake Baikal and induces the anomalous cold and dry northerlies. In turn, these northerlies weaken the convective activity over North Korea, which finally results in the decreasing tendency of rainfall over this region in recent decades (Choi et al., 2010, 2013). Another possible mechanism is that northward movement of monsoon rain band results in changes of dry and wet conditions over the East Asia monsoon region based on future climate change scenarios (Lee et al., 2013; Xin et al., 2013), which is also in line with earlier studies based on the observation data (Si et al., 2009; Zhu et al., 2011, 2015). The area-averaged change in precipitation over South Korea is projected to increase by (12.2%, 9.2%) in the RCP4.5 scenario by the end of the (Fut1, Fut2) period and by (3.8%, 15.0%) in the RCP8.5 scenario. These results are consistent with

previous studies using WRF models (Hong and Ahn, 2015; Im et al., 2015) and the overall pattern of precipitation follows large-scale forcing not only in regional details but also in fine-scale weather features (Lee et al., 2014; Hong and Ahn, 2015).

In order to assess the level of consistency in annual-mean precipitation projected by 5 RCMs, we constructed a consistency index (Wang, 2005; Kim and Byun, 2009). The spatial distribution of the consistency index (in percentage) is shown in Fig. 4. The sign of the index indicates the direction of change predicted by the majority of the models. The changes for each grid point where more than 60% of the RCMs agree on the direction of change are regarded as robust changes. The level of consistency is especially high in projecting the increase in precipitation over the southern part of South Korea (34°N-36°N) in the two RCP scenarios for the whole period. Otherwise, the level of consistency over the northern part of South Korea (36°N-40°N) is characterized by strong variability with both positive and negative signs among the scenarios. In particular, the level of consistency over the northern part of South Korea exhibits a positive (negative) sign during Fut1 period in the RCP4.5 (RCP8.5) scenario and during Fut2 period in the RCP8.5 (RCP4.5) scenario. The area-averaged consistency indices over South Korea during Fut1 (Fut2) period are 99.1% (88.8%) and 39.5% (98.2%) in the RCP4.5 and RCP8.5 scenarios, respectively. These results indicate that the changes in precipitation for all scenarios (Fig. 3) do not reflect the extreme biases from certain models, especially in the southern part of South Korea.

Figure 5a shows the area-averaged annual-mean precipitation anomalies over South Korea as simulated in the HIS experiment for the period 1981-2010 and in the RCPs experiments for the period 2021-2100. The analysis method and domain used in Fig. 5 are similar to those of Im et al. (2015). However, their study is confined to the single RCM results. In this regard, it is necessary to further examine the characteristics of future precipitation using the MME projections derived from various RCMs to reduce the uncertainty. The anomalies are derived by subtracting the climatological mean of the HIS experiment from each simulation, so that systematic model biases are partly eliminated. In the case of the HIS experiment, the simulated mean precipitation represents the inter-annual variability and shows a weakly positive trend. In addition, the projected precipitation for Fut1 and Fut2 periods retains inter-annual and decadal-scale variability, which is in agreement with two previous studies using only WRF models (Ahn et al., 2014; Im et al., 2015). In particular, the simulated future precipitation anomaly for the RCP4.5 (RCP8.5) scenario becomes almost constant during Fut1 (Fut2) period, but exhibits a negative (positive) trend for Fut2 (Fut1) period.

In addition to the change in mean precipitation, trend analysis is also conducted to examine the intensity and frequency of precipitation (Figs. 5b, c). The simulated mean precipitation, intensity and frequency of precipitation have similar structures in the two RCPs, but the magnitudes differ

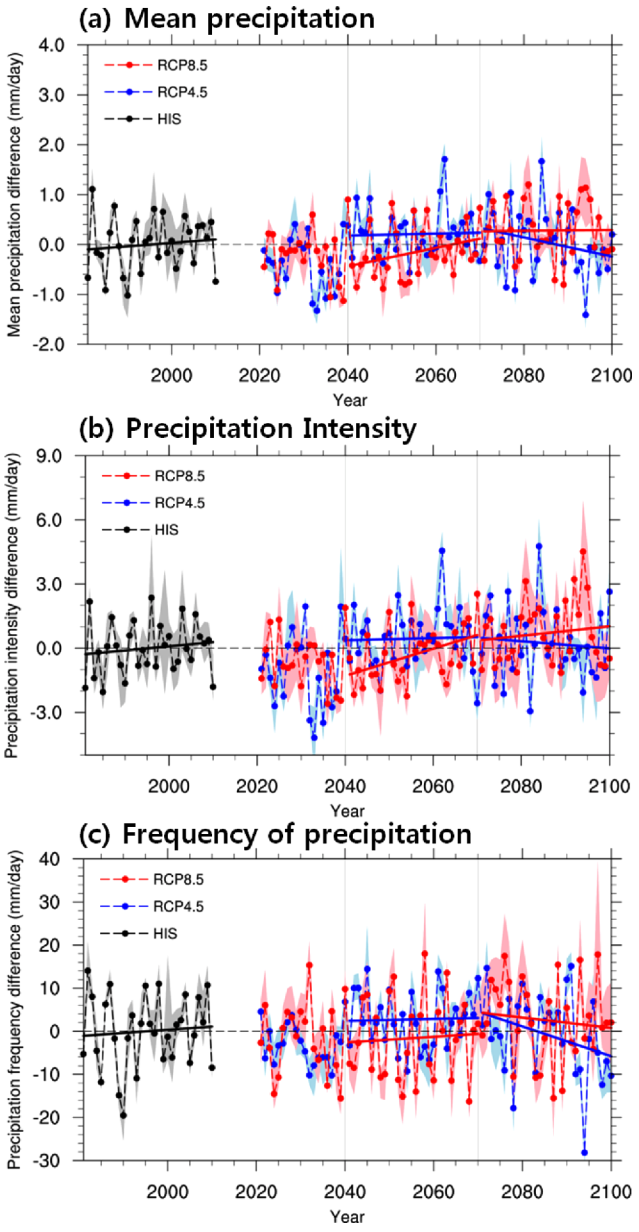

Fig. 5. Time-series of annually averaged anomalies of (a) mean precipitation, (b) intensity, and (c) frequency of monthly precipitation over South Korea against the historical (1981-2010) period. The dashed lines denote their trends for each period (1981-2010, 2041-2070, and 2071-2100). The shading indicates the ensemble spread in all panels.

depending on the GHG forcing and regions. In particular, the simulated intensity of precipitation for the RCP4.5 scenario becomes almost constant during Fut1, but shows a weakly decreasing trend for Fut2 period. On the other hand, the trend of simulated precipitation intensity for the RCP8.5 scenario increases over the time period (2021-2100). In addition to this, the simulated frequency of precipitation has a weakly positive trend for the Fut1 period, while it has a distinctive negative trend during the Fut2 period under the RCP4.5 and RCP8.5 scenarios. This implies that future changes in precipitation

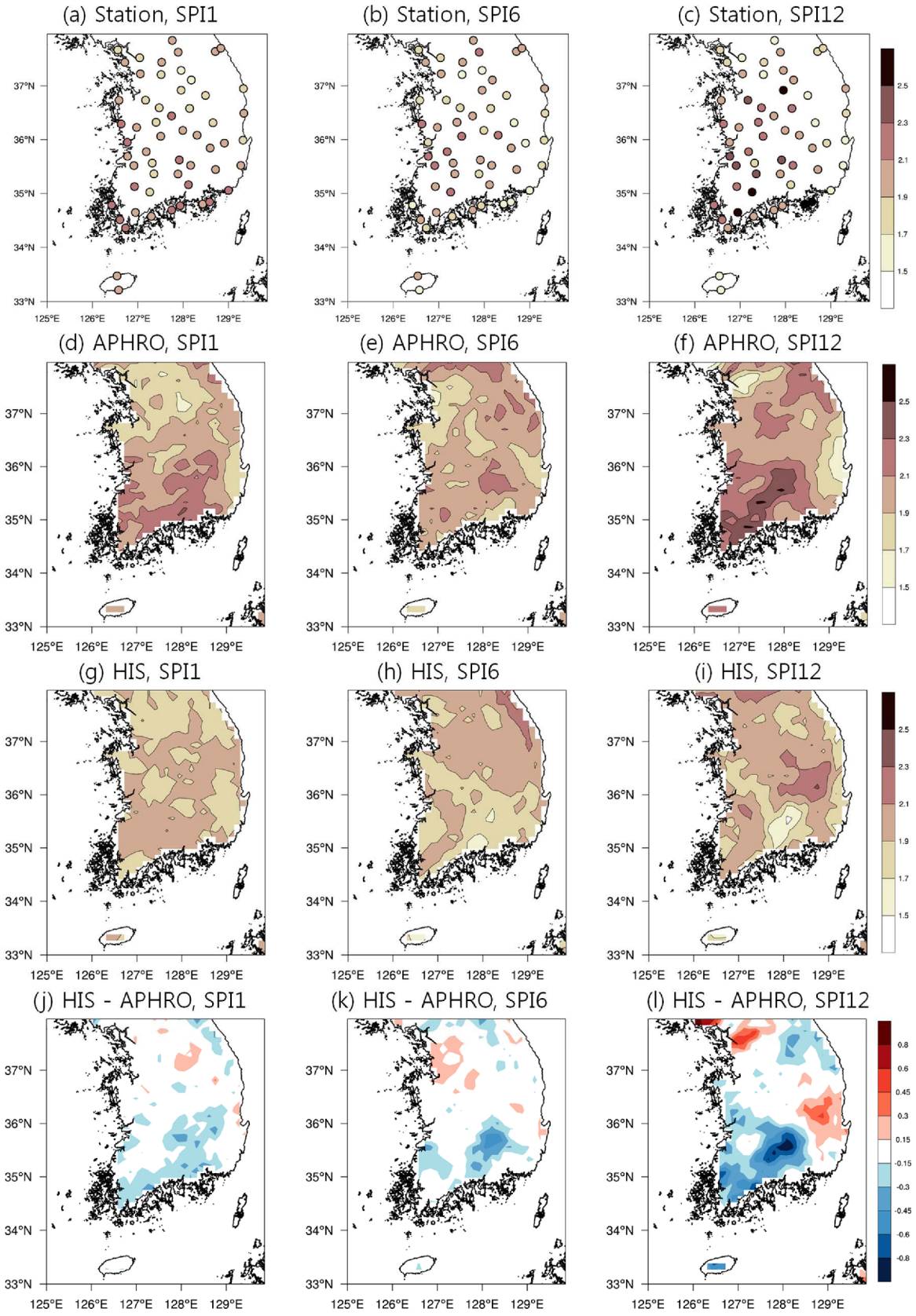

Fig. 6. Spatial distribution of the number of months (months/year) in which Standardized Precipitation Indices [(a, d, g) SPI1, (b, e, h) SPI6, and (c, f, i) SPI12] are less than −1 for (a, b, c) weather station data, (d, e, f) APHRODITE, (g, h, i) Ensemble of 5 RCMs, and (j, k, l) their differences between historical experiment and APHRODITE; Unit: fractions of a month.

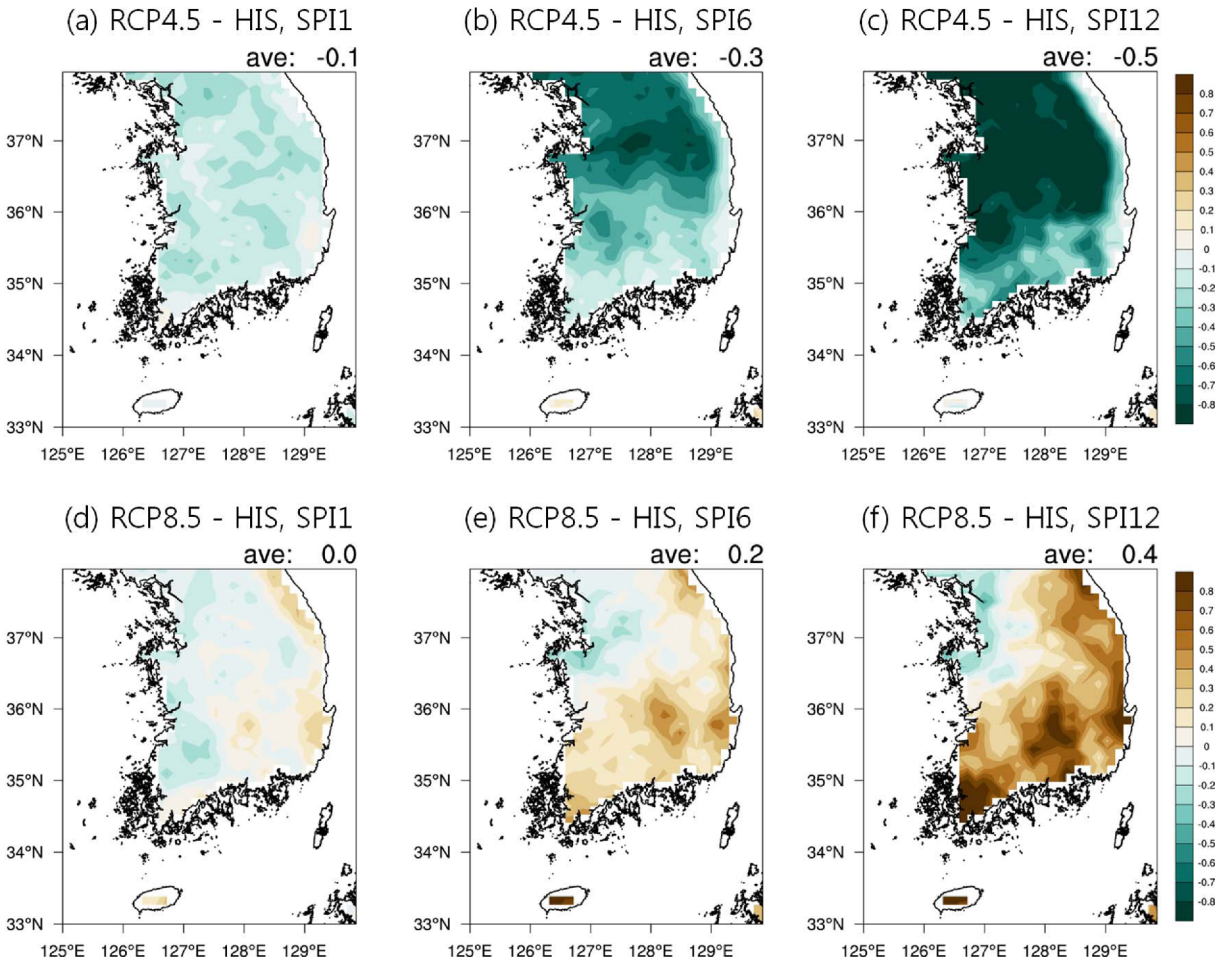

Fig. 7. Spatial distribution of the change in the number of months (months/year) in which Standardized Precipitation Indices [(a, d) SPI1, (b, e) SPI6 and (c, f) SPI12] are less than −1 for (a, b, c) RCP4.5 and (d, e, f) RCP8.5 experiments during Fut1 (2041-2070) period against the historical (1981-2010) period. The number at the top right of each panel indicates the averaged number of months over South Korea.

characteristics are inconsistent with the monotonic increase in temperature in the future scenarios, as they exhibit non-linear response to different emission scenarios.

c. Change in drought

The annual-mean number of drought months projected by the MME under HIS scenario is evaluated over South Korea against observations (Fig. 6). The condition for each grid point in which the SPIs are less than −1 is regarded as drought state. The spatial distribution of the number of drought months derived from three SPIs is shown in Fig. 6 using not only weather station data (Figs. 6a-c), but also APHRODITE (Figs. 6d-f). The spatial distribution of dry conditions derived from AHPRODITE overall follows a similar pattern to the station data. A large number of drought months are found over the southern part and northeastern coastal regions of South Korea in both sets of observations. Especially, the peak number of drought months is observed in the southwestern part of South Korea in SPI-12 case. These results denote that APHRODITE can appropriately capture the spatial distribution of the drought condition, regardless of the magnitude of SPIs. The simulated drought condition in the HIS experiment is, to some extent, similar to that of APHRODITE (Figs. 6g-i), but the comparison between the MME obtained from the five RCMs and APHRODITE shows large differences in the number of drought months over the southern part of South Korea, which become large as the duration of the drought increases (Figs. 6j-l). Although the MME has such a systematic bias in projecting dry conditions, it can be eliminated by subtracting the climatological mean of the HIS experiment from that of the RCP experiment. This evaluation provides an overview of the MME performance before projecting fine-resolution drought change on a regional scale.

To estimate the changes of drought frequency in the future, the MME differences in the number of drought months between the RCPs and HIS experiments are analyzed (Figs. 7 and 8). The number of drought months in the future will be characterized by strong variability, with both increasing and decreasing trends among the scenarios. In particular, the

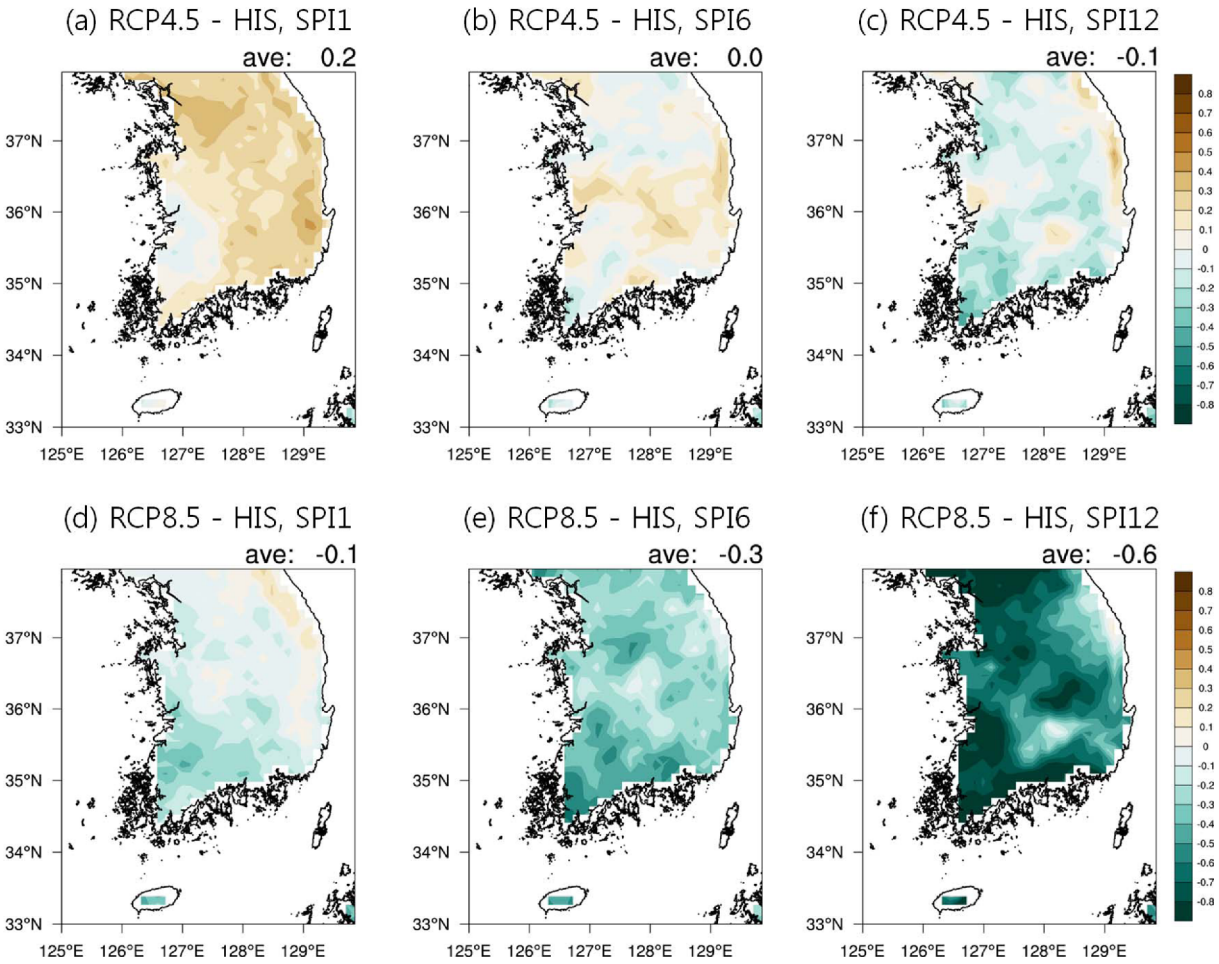

Fig. 8. Same as in Fig. 7 but for period from 2071 to 2100.

number of drought months over South Korea is projected to increase (decrease) during Fut1 period in the RCP8.5 (RCP4.5) scenario and increase (decrease) during Fut2 period in the RCP4.5 (RCP8.5) scenario, regardless of drought duration. These results coincide well with the results shown in Figs. 3, 4, and 5. Especially for SPI-1 and SPI-6, changes in the number of drought months are in good agreement with those in precipitation characteristics shown in Fig. 5. This means that weak precipitation, less amount and lower-frequency of precipitation can induce a large number of drought months, and vice versa. Another interesting feature is that the drought occurrence is expected to decrease in the future scenarios as the duration of the drought increases, except for the Fut1 period of the RCP8.5 scenario, during which 30-yr average of precipitation intensity and frequency are clearly projected to decrease in the mean sense.

In addition to the climatological change in the number of drought months, the trend analysis can provide some evidence for the response of drought to the emission forcing. Figure 9 shows a map of linear trends of SPIs. The positive and negative SPI values denote the wet and dry conditions, respectively. The SPI index becomes more negative (positive) as the dry (wet) condition becomes more severe. The most noticeable characteristic appearing in the trend analysis is that the SPIs are projected to gradually increase over South Korea during the entire future period, except for SPI-1 in the RCP4.5 scenario. In particular, SPI-1 under the RCP4.5 scenario shows no trend for 80 years (2021-2100), which is partly caused by the characteristics of the inter-decadal variability of the precipitation (Fig. 5). However, SPI-1 over the high mountainous region of South Korea shows a weakly negative long-term trend, which seems to be due to the negative long-term trends of precipitation frequency in the RCP4.5 scenario, as shown in Fig. 5c. Another interesting feature is that the SPIs are expected to increase in the future scenarios as the duration of the drought increases.

Figure 10 shows the anomalies of the annual percentage areas in drought conditions (SPIs < -1) over South Korea during 1981-2010 for the HIS experiment and during 2021-2100 for the RCPs experiment. The anomalies are derived by subtracting the climatological mean of the HIS experiment from each simulation. The most noticeable characteristic appearing in the trend analysis is that the drought areas are projected to gradually decrease over South Korea during the

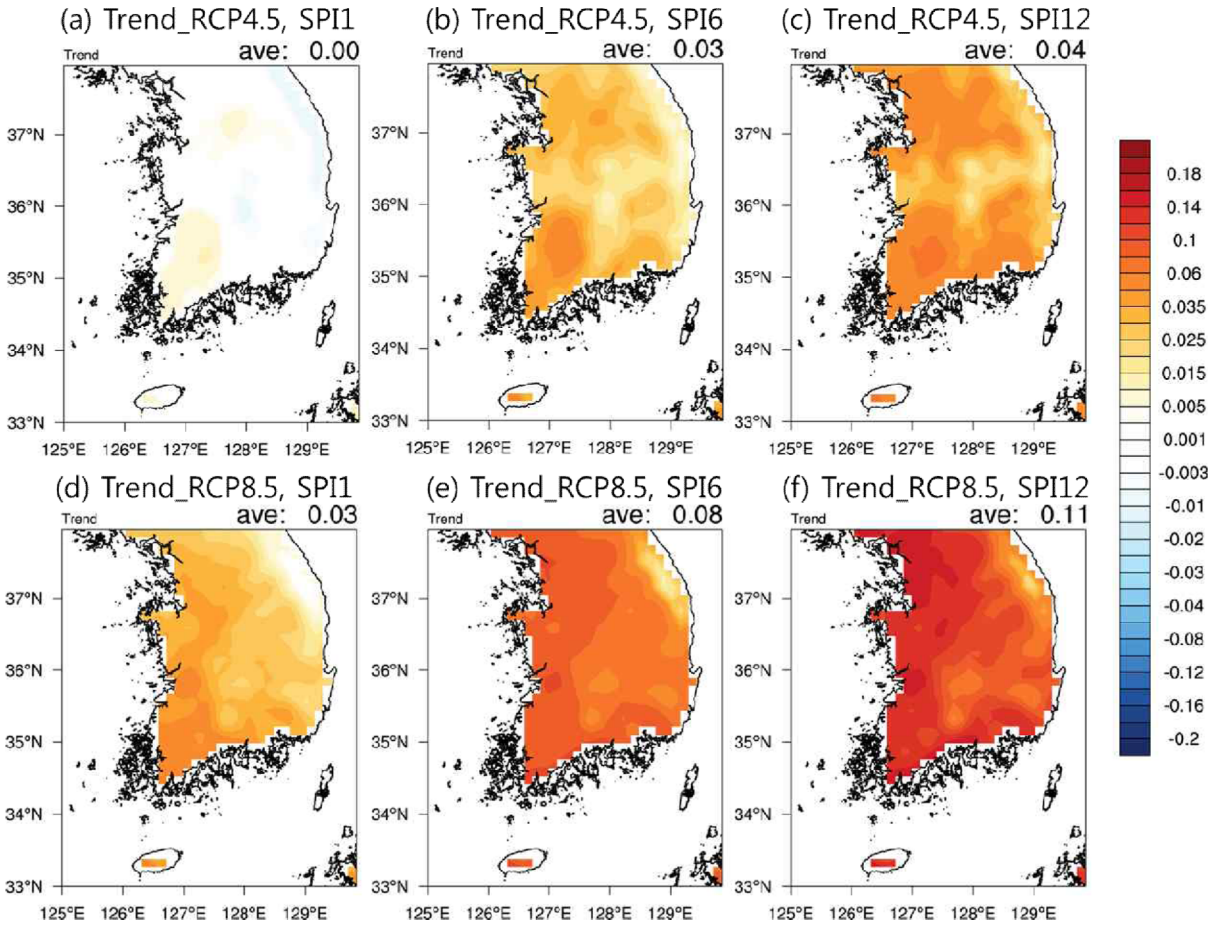

Fig. 9. Maps of linear trends of SPI (change per 10 years) during 2021-2100. Blue (Red) areas indicate drying (wetting) over South Korea.

entire future period, except for SPI-1 in the RCP4.5 scenario. In particular, the drought areas for SPI-1 in the RCP4.5 scenario show a weakly positive long-term trend, which is closely related to the negative long-term trends of mean precipitation and precipitation frequency in the RCP4.5 scenario, as shown in Figs. 5a, c. Otherwise, future changes in drought areas for SPI-6 and SPI-12 have a marked downward trend under the two RCP scenarios. Especially, the percentage areas of drought for SPI-12 have stronger negative trends than those of SPI-6. Furthermore, another noticeable characteristic appearing in the trend analysis of drought area is that the long-term drought has greater amplitude of variability than those of short-term drought. This result implies that South Korea will probably be wetter in the future according to the simulations, which accords well with the results from Fig. 9.

4. Summary and discussion

In this study, the projection of future drought conditions is estimated over South Korea based on the latest and most advanced sets of regional climate model simulations under the RCP4.5 and RCP8.5 scenarios, within the context of the national downscaling project of South Korea. The five RCMs were used to produce climate-change simulations around the Korean Peninsula and to analyze the uncertainty associated with these simulations. The horizontal resolution of each RCM is 12.5 km and model simulations are available for HIS (1981-2010) and future (2021-2100) periods under forcing from the RCP4.5 and RCP8.5 scenarios.

The performance of the HadGEM2-AO and MME in reproducing the precipitation and drought conditions in the HIS experiment is evaluated against observations over South Korea. The results show that the MME can not only reproduce the proper spatial distribution of the precipitation, particularly in the regions where orographically induced precipitation prevails, but also reasonably reproduce drought conditions in the region.

In the future scenarios, the mean precipitation is projected to consistently increase over the southern part of South Korea (34°N-36°N), whereas the sign of projected precipitation change over the northern part of South Korea (36°N-40°N) differs depending on the period and RCP scenarios. In particular, mean precipitation over the northern part of South Korea is projected to increase during Fut1 period in RCP4.5 and during Fut2 period in RCP8.5 scenario, but decrease during Fut1 period in the RCP8.5 scenario and during Fut2 period in

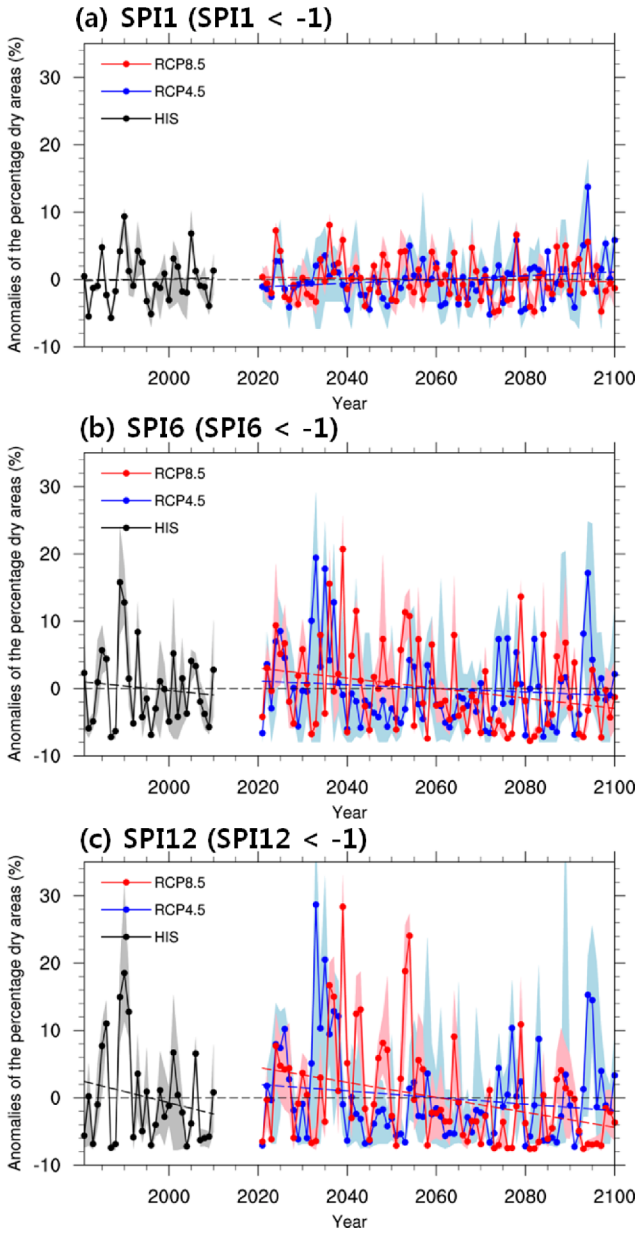

Fig. 10. Time series of anomalies (relative to 1981-2010) of annual percentage areas in drought conditions with SPI indices [(a) SPI1, (b) SPI6 and (c) SPI12] < −1 over South Korea against the historical (1981-2010) period. The shading indicates ensemble spread in all panels.

the RCP4.5 scenario. These results are consistent with previous studies utilizing WRF models (Hong and Ahn, 2015; Im et al., 2015) and the overall pattern of precipitation follows large-scale forcing with not only regional details but also fine-scale weather features (Lee et al., 2014; Hong and Ahn, 2015).

Trend analysis is conducted to examine the future change in mean precipitation, as well as the intensity and frequency of precipitation (Fig. 5). The characteristics of the simulated precipitation in terms of mean precipitation, intensity and frequency of precipitation under the RCP4.5 scenario become almost constant during Fut1 period, but show a negative trend during Fut2 period. Meanwhile, the evolving patterns of precipitation under the RCP8.5 scenario contain mixed features compared to the RCP4.5 scenario. The trend of simulated precipitation characteristics under the RCP8.5 scenario increases during Fut1 period, while the simulated mean precipitation becomes almost constant during Fut2 period. In addition, the intensity and frequency of precipitation under the RCP8.5 scenario show increasing and decreasing trends for Fut2 period, respectively.

The annual-mean number of drought months (SPIs < −1) projected by the MME under HIS scenario is evaluated over South Korea against observations (Fig. 6). The simulated drought condition in the HIS experiment has a similar spatial distribution to that of APHRODITE over South Korea. According to the MME differences in the number of drought months between the RCPs and HIS experiments, the number of drought months in the future will be characterized by strong variability, with both increasing and decreasing trends among the scenarios. In particular, the number of drought months over South Korea is projected to increase (decrease) during Fut1 period in the RCP8.5 (RCP4.5) scenario and increase (decrease) during Fut2 period in the RCP4.5 (RCP8.5) scenario, regardless of drought duration. These results coincide well with the results shown in Figs. 3, 4, and 5. Especially for SPI-1 and SPI-6, changes in the number of drought months are in good agreement with those of the precipitation characteristics such as mean, intensity and frequency. This means that weak precipitation, less amount and lower frequency of precipitation can induce a large number of drought months, and vice versa. Another interesting feature is that the drought occurrence is expected to decrease in the future scenarios as the duration of the drought increases, except for the RCP8.5 scenario during Fut1 period, in which 30-yr average of precipitation intensity and frequency are clearly projected to decrease in the mean sense.

In addition to the climatological change in the number of drought months, the trend analysis can provide some evidence for the response of drought to the emission forcing. The most noticeable characteristic appearing in the trend analysis is that the drought areas are projected to gradually decrease over South Korea during the entire future period, except for SPI-1 in the RCP4.5 scenario. In particular, the drought areas for SPI-1 in the RCP4.5 scenario show a weakly positive long-term trend, which is closely related to the negative long-term trends of mean precipitation and precipitation frequency in the RCP4.5 scenario. Otherwise, future changes in the drought areas for SPI-6 and SPI-12 have a marked downward trend under the two RCP scenarios. Especially, the percentage areas of drought for SPI-12 have stronger negative trends than those of SPI-6. Furthermore, another noticeable characteristic appearing in the trend analysis of the drought area is that the long-term droughts have greater amplitude of variability than those of short-term drought.

This study has assessed the future changes in drought

characteristics over South Korea using multi regional climate models with multiple time-scale SPIs, which have been widely used in recent years because of their computational simplicity and reliable interpretation. However the limitations of this study are that SPI is only based on precipitation without considering other variables such as temperature and evapotranspiration, which also play important roles in the drought variability, in particular under the global warming background (Chen and Sun, 2015a, 2015b). In addition, although these projected climate changes using 1 GCM and 5 RCMs model-chain still have uncertainties arising from GHG forcing scenarios, lateral boundary conditions, physical parameterization, and the selected models (global and/or regional), we expect these results to serve as the basis for understanding the future drought characteristics on multiple time scales over this region. Further studies for ensemble projection using diverse CGCMs and regional climate models are necessary to provide a more reliable climate projection.

Acknowledgements. This work was funded by the Korea Meteorological Administration Research and Development Program under grant KMIPA 2015-2081 and the Rural Development Administration Cooperative Research Program for Agriculture Science and Technology Development Project PJ009953.

Edited by: John McGregor

References

Ahn, J.-B., J.-L. Lee, and E.-S. Im, 2012: The reproducibility of surface air temperature over South Korea using dynamical downscaling and statistical correction. *J. Meteor. Soc. Japan*, **90**, 493-507.

_____, Y.-W. Choi, S.-R. Jo, and J.-Y. Hong, 2014: Projection of 21st century climate over Korean Peninsula: temperature and precipitation simulated by WRFV3.4 based on RCP4.5 and 8.5 scenarios. *Atmosphere*, **24**, 541-554 (in Korean with English abstract).

_____, J.-Y. Hong, and K.-M. Shim, 2015: Agro-climate changes over Northeast Asia in RCP scenarios simulated by WRF. *Int. J. Climatol.,* **36**, 1278-1290.

Baek, H.-J., and Coauthors, 2013: Climate change in the 21st century simulated by HadGEM2-AO under representative concentration pathways. *Asia-Pac. J. Atmos. Sci.*, **49**, 603-618.

Beniston, M., and Coauthors, 2007: Future extreme events in European climate: an exploration of regional climate model projections. *Climatic Change*, **81**, 71-95.

Blenkinsop, S., and H. J. Fowler, 2007: Changes in European drought characteristics projected by the PRUDENCE regional climate models. *Int. J. Climatol.*, **27**, 1595-1610.

Bothe, O., K. Fraedrich, and X. Zhu, 2012: Precipitation climate of Central Asia and the large-scale atmospheric circulation. *Theor. Appl. Climatol.*, **108**, 345-354.

Cha, D.-H., D.-K. Lee, and S.-Y. Hong, 2008: Impact of boundary layer processes on seasonal simulation of the East Asian summer monsoon using a regional climate model. *Meteor. Atmos. Phys.*, **100**, 53-72.

_____, and D.-K. Lee, 2009: Reduction of systematic errors in regional climate simulations of the summer monsoon over East Asia and the western North Pacific by applying the spectral nudging technique. *J. Geophys. Res.*, **114**, D14108, doi:10.1029/2008JD011176.

Chen, H. P., and J. Q. Sun, 2015a: Drought response to air temperature change over China on the centennial scale. *Atmos. Oceanic Sci. Lett.*, **8**, 113-119.

_____, and _____, 2015b: Changes in drought characteristics over China using the standardized precipitation evapotranspiration index. *J. Climate*, **28**, 5430-5447.

Choi, K.-S., S.-B. Oh, D.-W. Kim, and H.-R. Byun, 2010: The south-north oscillation centered on 1996 in Korean summer rainfall variability. *Atmosphere*, **20**, 91-100 (in Korean with English abstract).

_____, S.-D. Kang, and H.-D. Kim, 2013: Interdecadal change in North Korean winter mean rainfall. *Theor. Appl. Climatol.*, **114**, 169-182.

Chung, Y.-S., and M.-B. Yoon, 2000: Interpretation of recent temperature and precipitation trends observed in Korea. *Theor. Appl. Climatol.*, **67**, 171-180.

_____, _____, and H.-S. Kim, 2004: On climate variations and changes observed in South Korea. *Climatic Change*, **66**, 151-161.

Collins, W. J., and Coauthors, 2011: Development and evaluation of an earth-system model - HadGEM2. *Geosci. Model Dev.,* **4**, 997-1062.

Dai, A., K. E. Trenberth, and T. Qian, 2004: A global dataset of Palmer drought severity index for 1870-2002: Relationship with soil moisture and effects of surface warming. *J. Hydrometeor.*, **5**, 1117-1130.

_____, 2011: Drought under global warming: a review. *Wiley Interd. Rev. Clim. Change*, **2**, 45-65.

Davies, T., M. J. P. Cullen, A. J. Malcolm, M. H. Mawson, A. Staniforth, A. A. White, and N. Wood, 2005: A new dynamical core for the Met Office's global and regional modelling of the atmosphere. *Quart. J. Roy. Meteor. Soc.*, **131**, 1759-1782.

Giorgi, F., and X. Bi, 2005: Updated regional precipitation and temperature changes for the 21st century from ensembles of recent AOGCM simulations, *Geophys. Res. Lett.*, **32**, L21715, doi:10.1029/2005GL02-4288.

_____, and E. Coppola, 2010: Does the model regional bias affect the projected regional climate change? An analysis of global model projections. *Climatic Change*, **100**, 787-795.

_____, E. S. Im, E. Coppola, N. S. Diffenbaugh, X. J. Gao, L. Mariotti, and Y. Shi, 2011: Higher hydroclimatic intensity with global warming. *J. Climate*, **24**, 5309-5324.

_____, and Coauthors, 2012: RegCM4: model description and preliminary tests over multiple CORDEX domains. *Clim. Res.*, **52**, 7-29.

Guttman, N. B., 1998: Comparing the Palmer drought index and the standardized precipitation index. *J. Am. Water Resour. As.*, **34**, 113-121.

Hayes, M. J., M. D. Svoboda, D. A. Wilhite, and O. V. Vanyarkho, 1999: Monitoring the 1996 drought using the standardized precipitation index. *Bull. Amer. Meteor. Soc.*, **80**, 429-438.

_____, M. Svoboda, N. Wall, and M. Widhalm, 2011: The Lincoln declaration on drought indices: universal meteorological drought index recommended. *Bull. Amer. Meteor. Soc.*, **92**, 485-488.

Hong, J.-Y., and J.-B. Ahn, 2015: Changes of early summer precipitation in the Korean Peninsula and nearby regions based on RCP simulations. *J. Climate*, **28**, 3557-3578.

Hong, S.-Y., M. Kanamitsu, J. E. Kim, and M. S. Koo, 2012: Effects of diurnal cycle on a simulated asian summer monsoon. *J. Climate*, **25**, 8394-8408.

_____, and Coauthors, 2013: The Global/Regional Integrated Model system (GRIMs). *Asia-Pac. J. Atmos. Sci.*, **49**, 219-243.

Hulme, M., Zhao Zhongci, and T. Jiang, 1994: Recent and future climate change in East Asia. *Int. J. Climatol.*, **14**, 637-658.

Hur, J., and J.-B. Ahn, 2014: The change of first-flowering date over South Korea projected from downscaled IPCC AR5 simulation: peach and pear. *Int. J. Climatol.*, **35**, 1926-1937.

_____, and _____, 2015: Seasonal prediction of regional surface air temperature and first-flowering date over South Korea. *Int. J. Climatol.,*

35, 4791-4801.

Im, E.-S., _____, and D.-W. Kim, 2012: An assessment of future dryness over Korea based on the ECHAM5-RegCM3 model chain under A1B emission scenario. *Asia-Pac. J. Atmos. Sci.*, **48**, 325-337.

_____, _____, and S.-R. Jo, 2015: Regional climate projection over South Korea simulated by the HadGEM2-AO and WRF model chain under RCP emission scenarios. *Clim. Res.*, **63**, 249-266.

Kang, H., and S.-Y. Hong, 2008: An assessment of the land surface parameters on the simulated regional climate circulations: The 1997 and 1998 East Asian summer monsoon cases. *J. Geophys. Res.*, **113**, D15121, doi:10.1029/2007JD009499.

Kim, D.-W., and H.-R. Byun, 2009: Future pattern of Asian drought under global warming scenario. *Theor. Appl. Climatol.*, **98**, 137-150.

Ko, J.-W., H,-J. Baek, and W.-T. Kwon, 2005: The characteristics of precipitation and regionalization during rainy season in Korea. *Asia-Pac. J. Atmos. Sci.*, **41**, 101-114 (in Korean with English abstract).

Krishnamurti, T. N., C. M. Kishtawal, T. E. LaRow, D. R. Bachiochi, Z. Zhang, C. E. Williford, S. Gadgil, and S. Surendran, 1999: Improved weather and seasonal climate forecasts from multimodel super-ensemble. *Science,* **285**, 1548-1550.

Lee, D.-K., D.-H. Cha, and H.-S. Kang, 2004: Regional climate simulation of the 1998 summer flood over East Asia. *J. Meteor. Soc. Japan*, **82**, 1735-1753.

_____, D.-H. Cha, C.-S. Jin, and S.-J. Choi, 2013: A regional climate change simulation over East Asia. *Asia-Pac. J. Atmos. Sci.*, **49**, 655-664.

Lee, J.-W., and S.-Y. Hong, 2006: A numerical simulation study of orographic effects for a heavy rainfall event over Korea using the WRF model. *Atmosphere*, **16**, 319-332 (in Korean with English abstract).

_____, and _____, 2014: Potential for added value to downscaled climate extremes over Korea by increased resolution of a regional climate model. *Theor. Appl. Climatol.*, **117**, 667-677.

_____, S.-Y. Hong, E.-C. Chang, M.-S. Suh, and H.-S. Kang, 2014: Assessment of future climate change over East Asia due to the RCP scenarios downscaled by GRIMs-RMP. *Clim. Dynam.*, **42**, 733-747.

McKee, T. B., N. J. Doesken, and J. Kleist, 1993: The relationship of drought frequency and duration to time scales. *Proc. of the 8th Conf. on Applied Climatology*, Anaheim, CA, Amer. Meteor. Soc., 179-184.

Oh, S.-G., J.-H. Park, S.-H. Lee, and M.-S. Suh, 2014: Assessment of the RegCM4 over East Asia and future precipitation change adapted to the RCP scenarios. *J. Geophys. Res.,* **119**, 2913-2927.

Pal, J. S., and Coauthors, 2007: The ICTP RegCM3 and RegCNET: regional climate modeling for the developing world. *Bull. Amer. Meteor. Soc.*, **88**, 1395-1409.

Park, C., and Coauthors, 2015: Evaluation of multiple regional climate models for summer climate extremes over East Asia. *Clim. Dynam.*, **46**, 2469-2486.

Si, D., Y. H. Ding, and Y. J. Liu, 2009: Decadal northward shift of the Meiyu belt and the possible cause. *Chin. Sci. Bull.*, **54**, 4742-4748.

Skamarock, W. C., J. B. Klemp, J. Dudhia, D. O. Gill, D. M. Barker, W. Wang, and J. G. Powers, 2005: *A description of the advanced research WRF version 2.* NCAR/TN-468+STR, 88 pp.

_____, and Coauthors, 2008: *A description of the advanced research WRF version 3.* Tech. Note NCAR/TN-475+STR, 125 pp.

Solomon, S., D. Qin, M. Manning, Z. Chen, M. Marquis, K. B. Averyt, M. Tignor and H. L. Miller, Eds., 2007: *Climate Change 2007-The Physical Science Basis: Contribution of Working Group I to the Fourth Assessment Report of the Intergovernmental Panel on Climate Change*. Cambridge University Press, 1056 pp.

Trenberth, K. E., and Coauthors, 2014: Global warming and changes in drought. *Nat. Clim. Change,* **4**, 17-22.

Wang, G., 2005: Agricultural drought in a future climate: results from 15 global climate models participating in the IPCC 4th assessment. *Clim. Dynam.,* **25**, 739-753.

Xin, X., L. Zhang, J. Zhang, T. Wu, and Y. Fang, 2013: Climate change projections over East Asia with BCC_CSM1.1 climate model under RCP scenarios. *J. Meteor. Soc. Japan*, **91**, 413-429.

Yatagai, A., K. Kamiguchi, O. Arakawa, A. Hamada, N. Yasutomi, and A. Kitoh, 2012: APHRODITE: Constructing a long-term daily gridded precipitation dataset for Asia based on a dense network of rain gauges. *Bull. Amer. Meteor. Soc.*, **93**, 1401-1415.

Yun, W. T., L. Stefanova, and T. N. Krishnamurti, 2003: Improvement of the multimodel superensemble technique for seasonal forecasts. *J. Climate,* **16**, 3834-3840.

Zhu, Y. L., H. J. Wang, W. Zhou, and J. H. Ma, 2011: Recent changes in the summer precipitation pattern in east China and the background circulation. *Clim. Dynam.*, **36**, 1463-1473.

_____, H. Wang, J. Ma, T. Wang, and J. Sun, 2015: Contribution of the phase transition of pacic decadal oscillation to the late 1990s' shift in East China summer rainfall, *J. Geophys. Res.,* **120**, 8817-8827.